Desalination and Water Treatment
www.deswater.com
doi: 10.5004/dwt.2022.28367

256 (2022) 265–272
April

Photo-Fenton decolorization of dye with Cu solid state exchanged bentonite

Nahid Hajipour, Mohammad Ghorbanpour*, Atabak Feizi

Technical and Engineering Faculty, University of Mohaghegh Ardabili, Ardabil, Iran,
emails: Ghorbanpour@uma.ac.ir (M. Ghorbanpour), nahid.hajipour69@gmail.com (N. Hajipour),
a_feizi@uma.ac.ir (A. Feizi)

Received 31 August 2021; Accepted 2 March 2022

ABSTRACT

Bentonite/copper catalysts (CuB) were synthesized using solid-phase ion exchange at different temperatures (200°C and 300°C) and times (2 and 10 min) as heterogeneous catalysts for photo-Fenton treatment of methyl orange (MO) under UV irradiation. Prepared composites were identified by X-ray diffraction spectroscopy, scanning electron microscopy, Measurement of Brunauer–Emmett–Teller, transmission electron microscopy, energy-dispersive X-ray spectroscopy. The activity of the prepared CuB catalyst was assayed in the degradation of MO in the presence of the catalyst, H_2O_2, and UV irradiation. According to the decolorization of the MO solution, the sample prepared at 200°C and 10 min was selected as the optimal catalyst. Under optimal conditions (pH = 2.0, 30 mM H_2O_2, and 0.8 g/L catalyst), 100% of 100 ppm MO solution was removed at 135 min. The result of reusability studies shows the acceptable reusability of the catalyst.

Keywords: Discoloration; Bentonite; Copper; photo-Fenton; Solid-state ion exchange

1. Introduction

The photo-Fenton process is considered a high-efficiency wastewaters treatment method. The photo-Fenton process was conducted using H_2O_2, Fe^{2+}, and UV radiation [1,2]. In this process, $OH^{\bullet}$ was produced in ferrous Fe^{2+} and peroxide hydrogen (HP) as reductive and oxidative reagents, respectively. Produced hydroxyl radicals oxidized pollutants to CO_2 and H_2O, and other harmless substances. The photo-Fenton process is usually represented by Eqs. (1)–(3). The main reaction in the Fenton process is the Haber Weiss [Eq. (1)]:

$$Fe^2 + H_2O_2 \rightarrow Fe^{3+} + OH^- + HO \quad (1)$$

Fe^{3+} reduction through Eq. (2) also occurs, but the rate is considerably slower and is usually not considered:

$$Fe^{3+} + H_2O_2 \rightarrow Fe^{2+} + HO_2 + H^+ \quad (2)$$

The production of $HO^{\bullet}$ is greatly increased upon UV illumination by the photo-Fenton reaction [Eq. (3)] that closes the iron catalytic cycle:

$$Fe^{3+} + H_2O \rightarrow Fe^{2+} + HO^{\bullet} + H^+ \quad (3)$$

Since Fe^{2+} is regenerated [Eq. (3)] with the decomposition of water rather than H_2O_2 [Eq. (2)], the photo-Fenton process consumes less H_2O_2 and requires only catalytic amounts of Fe^{2+} [3]. Fast reaction rate, low chemical consumption, and removal capability of resistant pollutants are the significant advantages of this process [4]. Typically, most research was based on using iron catalysts [5,6]; however, some studies were done on the photo-Fenton properties of copper [7–9]. During the photo-Fenton process, catalysts can be used as homogeneous and heterogeneous [10]. Formation of metallic sludge leading

* Corresponding author.

to difficult catalyst separation is the major drawback of the homogeneous Fenton process. Thus, the replacement of the homogeneous catalysts with heterogeneous catalysts becomes an imperative alternative where the active metal can be incorporated into or onto a porous solid support. This replacement should preserve the activity of the catalyst and enhance its stability [5]. In this area, various materials such as clays, silica, and activated carbon have been studied [11,12], among which, clays represent an interesting option due to their low cost, abundance, and high surface area. Furthermore, their ion exchangeability is a good advantage leading to simple and easy preparation of catalyst/clay composites.

The incorporation of iron into clays can be done by different strategies. The simplest one may be the cationic exchange of the exchangeable cations of the clay, but this may lead to the contents of the cation being too low [1,8,9]. However, according to some recently published studies, these composites could be prepared by the solid-state ion exchange method [13–15]. Comparing the cationic exchange, the solid-state ion exchange is simpler, faster, and more cost-effective. In this method, clay is mixed with a salt of copper and heated by a furnace at a temperature close to the melting point of the salt. The molten salt penetrates the pores of clay, and ion exchange takes place in the molten salt medium. Hajipour et al. [14] prepared iron oxide/bentonite by the solid-state reaction method at 300°C and 600°C, where the degradation efficiency of methyl orange (MO) reached 81% and 75% in the presence of composite at 300°C and 600°C and H_2O_2 under 90 min irradiation. Finally, they concluded that the prepared catalysts method exhibit acceptable photo-Fenton catalytic activity. Rojas-Mantilla et al. [16] modified Brazilian natural clay by immobilizing iron oxide for heterogeneous Fenton degradation of the antibiotic sulfathiazole. They achieved high catalytic efficiency (>97% degradation after 60 min) with high stability and reusability. Shayegh and Ghorbanpour [15] prepared iron-pillared bentonite nanocomposite using a solid-state ion-exchange method to adsorb methylene blue dye. They observed that prepared samples showed a significant improvement in methylene blue dye removal capacity compared with parent bentonite.

According to the research, the photo-Fenton properties of solid state ion-exchanged bentonite with copper have not been studied yet.

2. Experimental

Bentonit (Ca-montmorillonite) was purchased from Kanisaz Jam Company (Rasht, Iran) and used as the adsorbent. Before the experiments, the bentonite was filtered to give a particle size of roughly 150 μm. $CuSO_4{\cdot}5H_2O$, chloride acid (HCl), hydrogen peroxide (H_2O_2), and methyl orange were purchased from Merck. All the compounds were used without further purification.

2.1. Copper exchanged bentonite

Bentonite (5 g) and $CuSO_4{\cdot}5H_2O$ (2.5 g) were completely mixed and heated at 200°C and 300°C for 2 and 10 min. Then, the mixture was adequately washed with distilled water. Finally, prepared copper-exchanged bentonite was filtered and dried in an oven for 24 h at 25°C.

2.2. Characterization

The X-ray diffraction (XRD) patterns of the samples were characterized using an X-ray diffractometer (Philips PW 1050, The Netherlands) with CuKα radiation (λ = 1.5418 Å, 40 kV and 30 mA, 2θ from 0 to 80° and 0.05° step). Scanning electron microscopy (SEM) and energy-dispersive X-ray spectroscopy (EDX) were carried out with an LEO 1430VP instrument. A Micromeritics Brunauer–Emmett–Teller (BET) surface area and porosity analyzer (Gemini 2375, Germany) evaluated the products with N_2 adsorption/desorption at the constant temperature of 77 K in the relative pressure range of 0.05–1.00.

2.3. Photo-Fenton activity

The photo-Fenton tests were carried out using a Pyrex open vessel (250 mL) containing 100 mL of the aqueous solution of MO (pH = 4, 150 ppm). This container was placed on a magnetic stirrer and irradiated with a UV lamp (UVC, 4 W, Philips). The distance between the surface of the solution and the UV source was kept constant at 15 cm, in all experiments. The prepared nanocomposites (0.8 g/L) and H_2O_2 (30 mM) were added to the reaction vessel. The moment of adding H_2O_2 was considered as the reaction initiation. During the reaction, the liquid aliquots were retrieved from the vessel at the selected periods and centrifuged. The dye removal efficiency was calculated as follows:

$$\text{Decolorization efficiency} = \left[\frac{C_0 - C_t}{C_t}\right] \times 100\% \quad (4)$$

where C_0 and C_t (ppm) are the concentration of the MO at the initial and any time t, respectively, measured by spectrophotometer.

3. Results and discussions

3.1. Characterization

The XRD patterns of parent bentonite (PB) and prepared composites (CuB) are shown in Fig. 1. The XRD pattern of PB indicates the presence of montmorillonite associated with quartzes and kaolinite. Upon solid-state ion exchange, the d-spacing calculated for the montmorillonite phase decreases from 14.07 Å in the PB to lower amounts (Table 1). According to Table 1, the decrease in d-spacing further decreases with increasing temperature and time. It has the lowest value in the sample prepared at a temperature of 300 for 10 min. According to available reports, this is due to water evaporation in the bentonite structure during the solid-phase ion exchange process [13,15]. The peak at 2θ = 6.30° corresponds to the d_{001} basal spacing of 1.40 nm that is typical of calcium-rich montmorillonites. The main peak in the XRD pattern of bentonite; appeared at 36.82° and the peak at 20.08°, corresponding to the structural feature of smectites [17]. Also, the peaks at 2θ = 21.01°, 26.80°, and 42.73° are

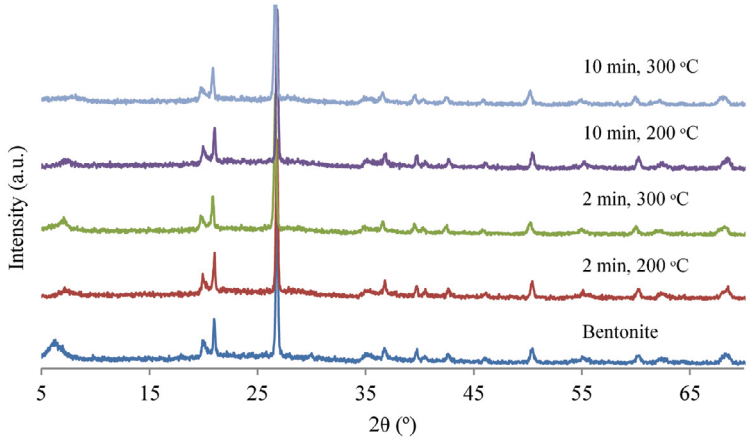

Fig. 1. The XRD patterns of PB and prepared composites.

Table 1
d-spacing of PB and prepared composites

Time of ion exchange (min)	PB	2		10	
Temperature of ion exchange (°C)		200	300	200	300
d-spacing (nm)	14.0706	12.2893	12.4759	11.887	10.4666

related to the quartz mineral in bentonite [18]. Relative changes in the peak positions and peak intensities in the Cu exchanged samples indicate that Cu atoms are well incorporated in the bentonite matrix. Fig. 1 the Cu exchanged samples show the diffraction peaks located at 36.39°, 43.04°, 50.04°, and 73.49° that can be assigned to Cu nanoparticles [19]. On the other hand, no copper-related phases are observed in the XRD patterns of composites pointing to high dispersion of the Cu in the composites [5,9].

To comprehend the elemental composition of the PB and the variations of ion exchange of copper, elemental analysis was performed on all the samples using EDX analysis. The obtained results is presented in Fig. 2. The chemical composition of PB and CuB are summarized in Table 2. The results revealed the high copper content and decreased calcium content in ion-exchanged samples compared to the PB. In other words, bentonite does not contain copper, while all ion exchange samples contain this element. Conversely, ion-exchange samples do not comprise any calcium, while bentonite comprises it. Besides, by increasing the temperature and time of the ion exchange process, the amount of ion-exchanged copper with calcium increases.

BET analysis of PB and CuB is presented in Table 3. The surface area decreases from 85 m^2/g for bentonite to lower amounts (between 55–70 m^2/g) due to the solid-state ion exchange process, pointing to a certain extent of pore blockage. However, a lower reduction of the surface area of the composite can be observed at 300°C. It seems that at higher temperatures, the copper particles formed due to the higher diffusion coefficient can be well diffused into the inner parts of the pores; therefore, the pore blockage is reduced. On the other hand, bentonite layers are more open at higher temperatures. Thus, a higher surface area and porosity of bentonite can be expected with higher temperatures. In any case, the values of the surface area are very similar to those previously reported for similar composites [7,20].

The morphology of the PB and CuB is shown in Fig. 2. A typical configuration of the bentonite with a sheet-like structure and large flakes is observed in Fig. 2a. The ion exchange of Cu into the bentonite seems not to have any noticeable change in the original apparent structure of

Table 2
Elemental analysis of PB and prepared composites

Time of ion exchange (min)	PB	2		10	
Temperature of ion exchange (°C)	Bentonite	200	300	200	300
Calcium	1.05	0	0	0	0
Potassium	1.17	0.93	0.64	0.94	0.74
Copper	0	1.01	1.68	1.65	1.86

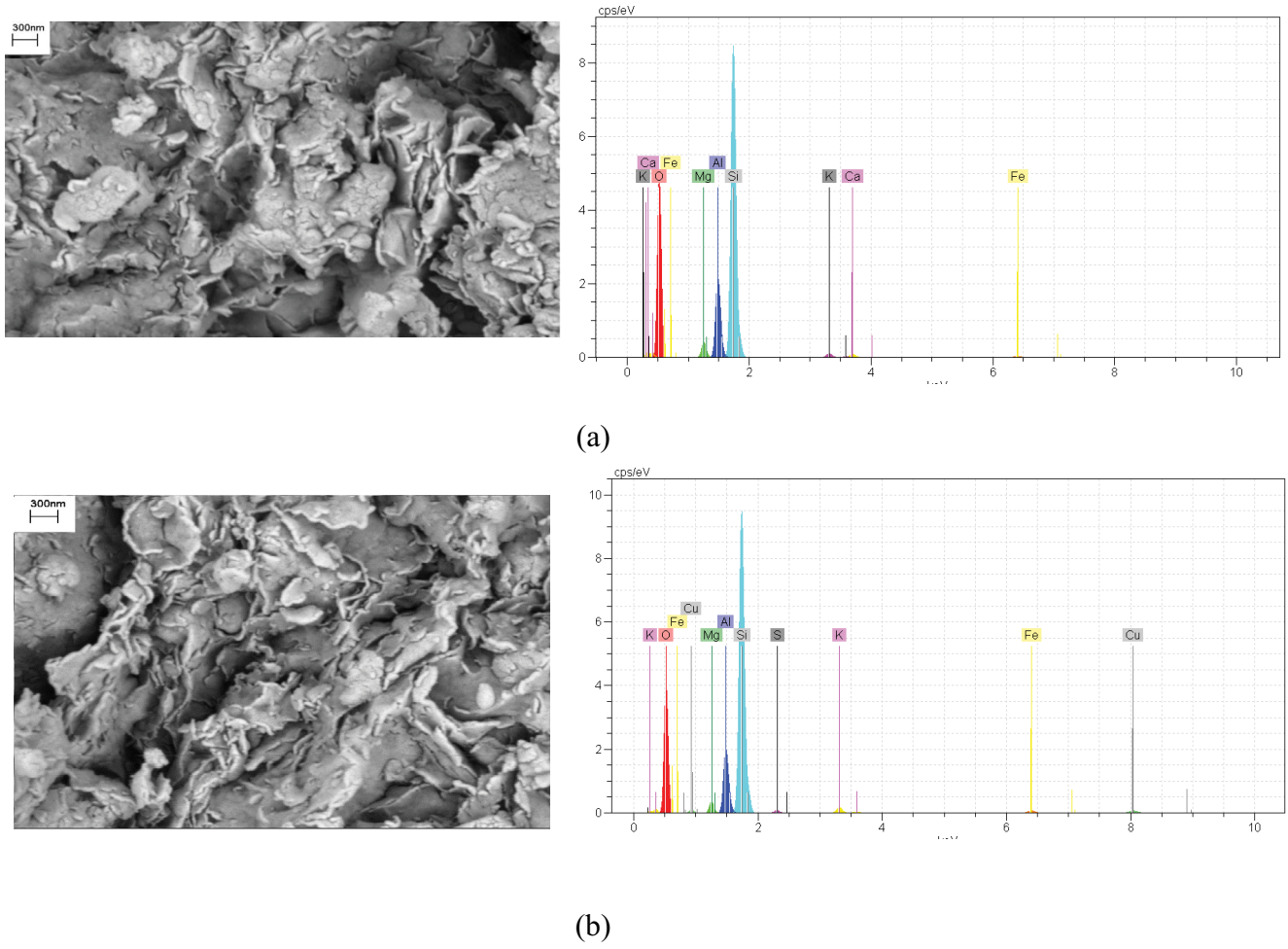

Fig. 2. SEM images and EDX analysis of PB (a) and CuB at 300°C for 2 min (b).

Table 3
BET analysis of PB and prepared composites

Time of ion exchange (min)	PB	2		10	
Temperature of ion exchange (°C)		200	300	200	300
Specific surface (m^2/g)	85.04	55.53	64.084	55.546	69.72
Total pore volume (cm^3/g)	0.1142	0.132	0.1363	0.1377	0.1581
Mean pore diameter (nm)	1.66	1.66	1.66	1.66	1.66

bentonite. No nanoparticles were formed on the surface of bentonite; however, based on elemental analysis, there is copper in bentonite. It may be due to the formation of copper oxide nanoparticles in the interlayer space of bentonite.

Fig. 3 shows the transmission electron microscopy (TEM) image of CuB at 200°C for 10 min. The TEM image proves that the synthesis method of CuB has been successful, and the copper oxide nanoparticles have been able to enter the nanometer distance between the clay plates in 10 min at temperature 200°C. The darker parts of the images show copper oxide nanoparticles, which are denser and restrict the passage of electrons [21].

3.2. Photo-Fenton activity

In this study, the methyl orange photocatalytic discoloration was studied as a model dye. The results showed that the discoloration efficiency of the synthesized catalysts at different times and temperatures is different (Fig. 4). Comparing the discoloration efficiency, the amounts of discoloration for ion-exchanged samples prepared at 200°C for 2 and 10 min were 62% and 78%, respectively. However, this efficiency was 66% and 77% for ion-exchanged samples prepared at 300°C for 2 and 10 min, respectively. It was found that the decolorization efficiency increased in a longer preparation time at

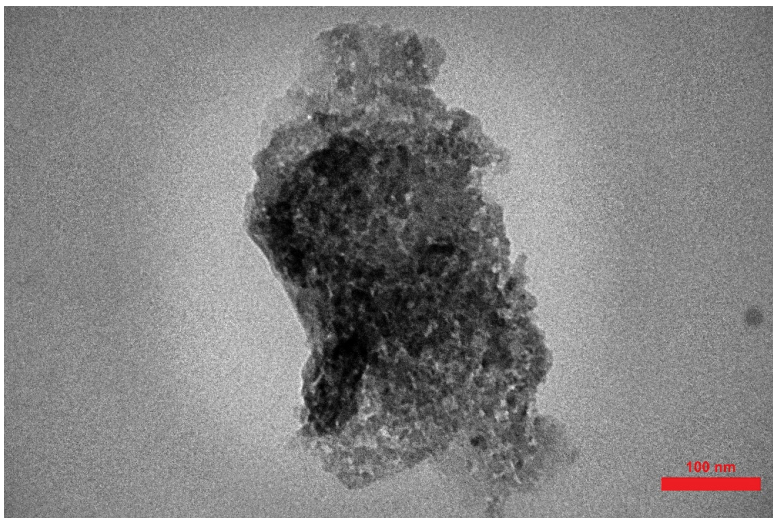

Fig. 3. TEM image of CuB at 200°C for 10 min.

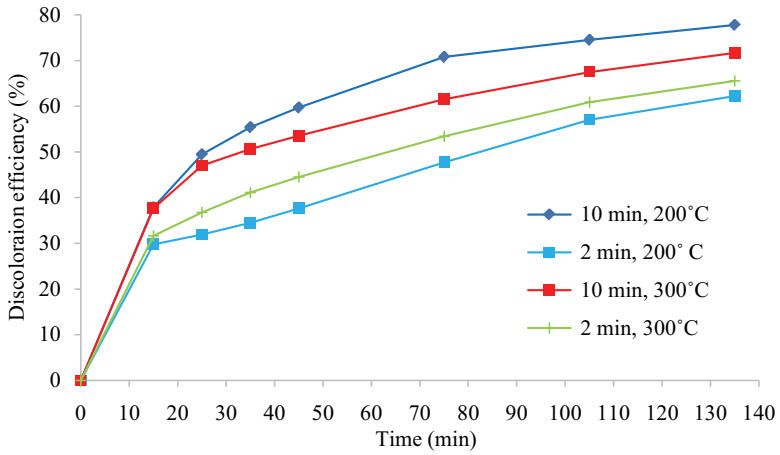

Fig. 4. Catalytic discoloration efficiencies of methyl orange by CuB.

each temperature. However, the higher ion-exchanged temperature has an inverse effect on the decolorization efficiency. The sample prepared at 200°C for 10 min was selected as the optimum sample.

The influence of the pH of the initial dye solution on the photo-Fenton activity of the catalyst was tested at pHs within the range of 2–8 in the presence of 0.8 g/L catalysts, UV irradiation, and H_2O_2. The results are presented in Fig. 5, indicating that the variation of the solution pH has a significant influence on the discoloration of dye. It is observed that with increasing pH, the decolorization percentage decreases. At acidic pH, the rate of degradation of hydrogen peroxide increases because the solubility of ferrous ions and the oxidizing power of hydroxyl radicals is higher. Similar observations have also been recently reported in the literature about the ability of Cu-based catalysts to generate hydroxyl radicals, referred to as a Fenton-like process [7,20]. Also, the low degradation at high pH could be explained because in the basic medium, the oxidizing species hydroperoxy anion (H_2O^-) was formed (which is the conjugate base of H_2O_2). The anion H_2O^- can react with both the hydroxyl radical and H_2O_2, decreasing the dye Eqs. (5) and (6) [22].

$$H_2O + H_2O^- \rightarrow H_2O + O_2 + OH^\bullet \quad (5)$$

$$OH^\bullet + H_2O^- \rightarrow H_2O + O_2^- \quad (6)$$

Fig. 6 shows the results of the photo-Fenton experiments conducted for H_2O_2 dosages from 15 mL to 35 mM, at a pH of 2, in the presence of 0.8 g/L catalysts and UV irradiation. The results point to the presence of an optimal oxidant dosage. It was observed that by increasing the amount of H_2O_2 from 15 mL to 30 mM, the $^\bullet$OH radical concentration increases. Hence, the rate of discoloration of dye also increases. It also occurs by increasing the amount of H_2O_2 generating per hydroxyl radicals at high H_2O_2 concentration, that is, beyond 0.30 mM scavenging of hydroxyl radical. Perhydroxyl radical is a less strong oxidant compared to hydroxyl radical. Therefore, the rate of dye discoloration decreases by increasing the

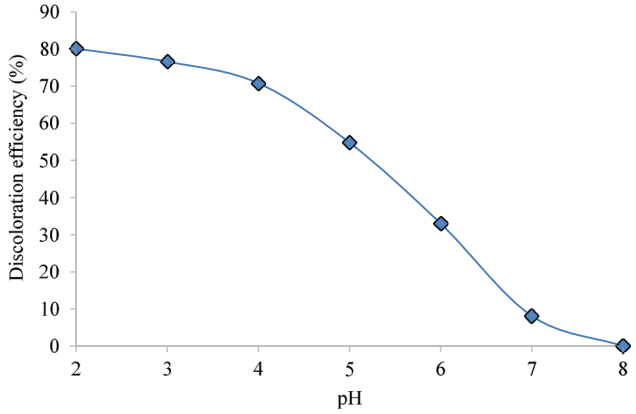

Fig. 5. Effect of the pH dosages on the photo-Fenton activity of CuB.

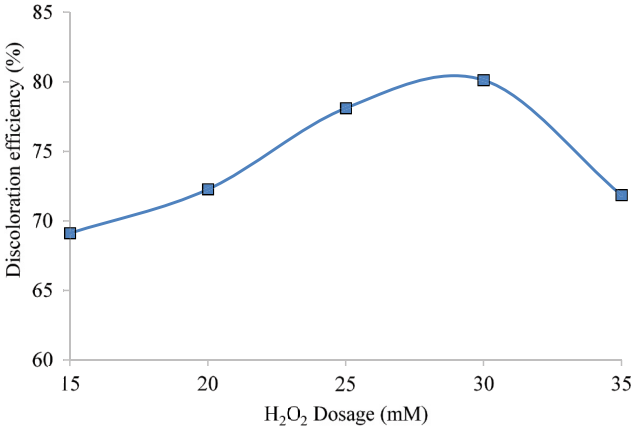

Fig. 6. Effect of the H_2O_2 dosages on the photo-Fenton activity of CuB.

amount of H_2O_2 beyond 30 mM [8]. Also, decreased the percent degradation of dye due to the reaction of •OH radicals with H_2O_2, forming less reactive OOH radicals; in other words, it can be it can be demonstrated that the large amount of H_2O_2 also scavenging •OH radicals. This observation is in agreement with the previous literature [23].

The effect of the catalyst's dosage was evaluated by varying its concentration from 0.2 to 0.12 g/L at a pH of 2, in the presence of 30 mM H_2O_2 and UV irradiation (Fig. 7). Dye conversion increases by increasing catalyst concentrations within the range of 0.2–0.8 g/L. This may be explained by the fact that by increasing the amount of catalyst, the surface area of the catalyst will increase, resulting in an enhanced free hydroxyl radical generation. Conversion is dramatically decreased for catalyst dosages within the range of 0.8–0.12 g/L. Excess of the catalyst leads to the difficulty of diffusion of the UV irradiation through a more opaque suspension.

Fig. 9 shows the effect of different color concentrations on the decolorization efficiency. It is observed that increasing the color concentration from 100 to 200 ppm decreases the decolorization efficiency from 100% to 76% after 135 min. In high initial concentrations with constant

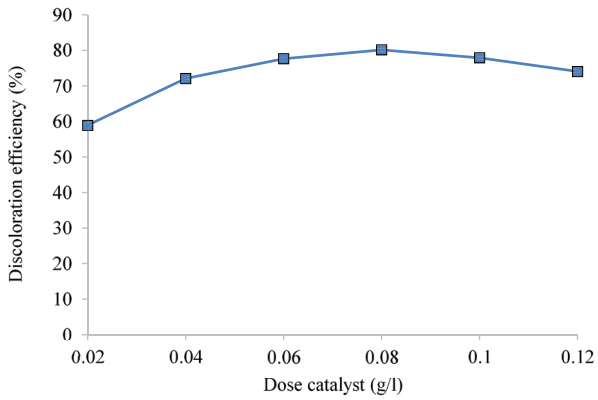

Fig. 7. Effect of the catalyst's dosage on the photo-Fenton activity of CuB.

radical hydroxyl concentration, the relative radical concentrations are low, which reduces [5].

The catalytic discoloration efficiencies of methyl orange by optimum composite were analyzed under different experimental conditions (Fig. 8). In this experiment, the concentration of H_2O_2, and the amount of catalyst were fixed at obtained optimum amounts, that is, 0.23 mL, and 0.8 g/L. The experiment was set at pH = 4. The discoloration kinetics of methyl orange is significantly influenced by the experimental conditions. Solely, UV irradiation results in near zero conversion. In the presence of the catalyst, maximal dye adsorption around 46% was measured. In the presence of H_2O_2, the dye solution, decolonization reaches 35%. The discoloration of 51% and 45% was achieved in the presence of catalyst or H_2O_2 under irradiation, respectively. H_2O_2 in the presence of catalyst results in 54% discoloration. The highest conversion of dye, close to 78%, was found when methyl orange was degraded in the presence of the catalyst, the oxidant H_2O_2, and UV irradiation. Using solid ion exchanged bentonite with iron, Isalou and Ghorbanpour [5] provided full dye removal of methylene blue solution (200 ppm) in the presence of hydrogen peroxide (30 mM) and catalyst (0.4 g/L) during 90 min at pH = 4 [5]. The results of the present work are comparable with their findings. In the present study, methyl orange solution (100 ppm) provided 100% efficiency in the presence of a much smaller amount of catalyst (0.8 g/L). Also, the reusability of the catalyst was performed in two stages. In the first and second stages, the removal efficiency of 100 ppm of the color solution was 85% and 79%, respectively. In another study, 98% of the dye solution (Rhodamine B) (19 ppm) was removed in the presence of hydrogen peroxide (0.12 mM) and a catalyst (0.2 g/L) at pH = 3 within 50 min. Although the type of dye was different from the present work, their dye concentration was lower, and the amount of catalyst was higher than the dye solution (Rhodamine B) of solution removed. Also after the first recycling, the activity of the catalyst was reduced from 98% to 66% [24]. Another study addressed the dye removal of Cu-pillared bentonite vs. 4-nitrophenol. Compared to the present laboratory work, they achieved 100% removal at an equal concentration and a higher amount of adsorbent (approximately 2.5 times

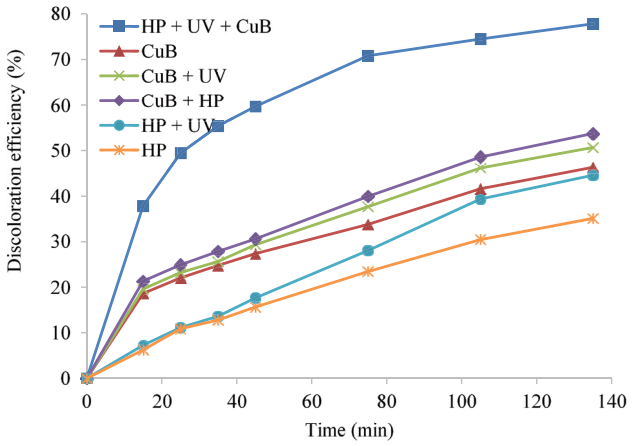

Fig. 8. Catalytic discoloration efficiencies of MO under different experimental conditions.

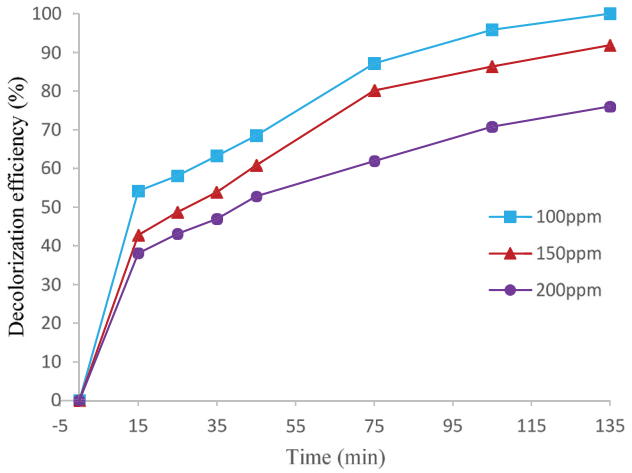

Fig. 9. Effect of MO initial concentration in optimal operating conditions.

greater). Besides, their synthesis was carried out at a temperature of 450°C, which is only 200°C and much easier in the present study [7].

3.3. Catalyst reusability

Fig. 10 represents the decolorization efficiencies after the second and third reuse of 85% and 79%, respectively. In contrast, this efficiency for first use was 100%. The reduction in the discoloration rate is attributed to the presence of the residual intermediate molecules in the discoloration of the methyl orange molecules on the photocatalyst surface, preventing the photon from reaching the photocatalyst surface. On the other hand, this decrease depends on the number of residual molecules on the catalyst surface. Accordingly, photocatalytic activity during these three periods has a relatively small difference. Moreover, the results show that it is possible to reuse the catalyst, which is essential for practical applications. The higher reusability of the catalyst can be related to the lamellar space present in the bentonite structure providing sufficient sites for Cu loading.

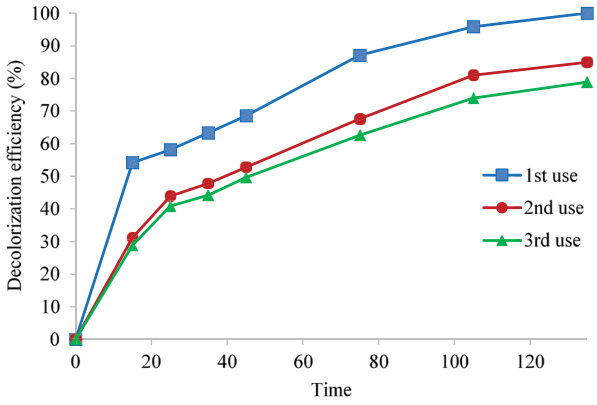

Fig. 10. Catalyst reusability after three use.

4. Conclusions

This study aimed to synthesize the catalyst by solid-phase ion exchange and identify and evaluate its photocatalytic activity. XRD spectroscopy showed that the d-spacing of bentonite decreased after the solid-phase ion exchange, and further decreased with increasing temperature and time. The surface area decreases from 85 m^2/g for bentonite to lower amounts (between 55–70 m^2/g) due to the solid-state ion exchange process. The EDX results revealed high copper content and decreased calcium content in ion-exchanged samples compared to the PB. According to SEM images, the ion exchange of Cu into the bentonite seems not to have any obvious change in the original apparent structure of bentonite. Optimal conditions for solid-phase ion exchange were obtained at 200°C and 10 min. Under optimal conditions (pH = 2.0, 30 mM H_2O_2, and 0.8 g/L catalyst), 100% of 100 ppm methyl orange solution was removed at 135 min. The resulting data showed the reusability of the synthesized catalyst. Thus, the solid-phase ion exchange catalyst synthesized with copper is an efficient catalyst for the photo-Fenton process.

References

[1] A.C.-K. Yip, F.L.-Y. Lam, X. Hu, Chemical-vapor-deposited copper on acid-activated bentonite clay as an applicable heterogeneous catalyst for the photo-Fenton-like oxidation of textile organic pollutants, Ind. Eng. Chem. Res., 44 (2005) 7983–7990.

[2] M.B. Kasiri, H. Aleboyeh, A. Aleboyeh, Modeling and optimization of heterogeneous photo-Fenton process with response surface methodology and artificial neural networks, Environ. Sci. Technol., 42 (2008) 7970–7975.

[3] C. Casado, J. Moreno-SanSegundo, I. De la Obra, B.E. García, J.A. Sánchez Pérez, J. Marugán, Mechanistic modelling of wastewater disinfection by the photo-Fenton process at circumneutral pH, Chem. Eng. Sci., 403 (2021) 126335, doi: 10.1016/j.cej.2020.126335.

[4] İ. Kıpçak, E.K. Ersal, Catalytic wet peroxide oxidation of a real textile azo dye Cibacron Red P-4B over Al/Fe pillared bentonite catalysts: kinetic and thermodynamic studies, React. Kinet. Mech. Catal., 132 (2021) 1003–1023.

[5] S.K. Isalou, M. Ghorbanpour, Catalytic activity of Fe-modified bentonite in heterogeneous photo-Fenton process, Desal. Water Treat., 162 (2019) 376–382.

[6] N. Silwana, B. Calderón, S.K.O. Ntwampe, A. Fullana, Heterogeneous fenton degradation of patulin in apple juice

using carbon-encapsulated nano zero-valent iron (CE-nZVI), Foods, 9 (2020) 674, doi: 10.3390/foods9050674.
[7] O.B. Ayodele, B.H. Hameed, Synthesis of copper pillared bentonite ferrioxalate catalyst for degradation of 4-nitrophenol in visible light assisted Fenton process, J. Ind. Eng. Chem., 19 (2013) 966–974.
[8] E. Kweinor Tetteh, E. Obotey Ezugbe, D. Asante-Sackey, E.K. Armah, S. Rathilal, Response surface methodology: photocatalytic degradation kinetics of Basic Blue 41 Dye using activated carbon with TiO_2, Molecules, 26 (2021) 1068, doi: 10.3390/molecules26041068.
[9] M. Rodríguez, J. Bussi, M.A. De León, Application of pillared raw clay-base catalysts and natural solar radiation for water decontamination by the photo-Fenton process, Sep. Purif. Technol., 259 (2021) 118167, doi: 10.1016/j.seppur.2020.118167.
[10] S. Xiao, M. Cheng, H. Zhong, Z. Liu, Y. Liu, X. Yang, Q. Liang, Iron-mediated activation of persulfate and peroxymonosulfate in both homogeneous and heterogeneous ways: a review, Chem. Eng. Sci., 384 (2020) 123265, doi: 10.1016/j.cej.2019.123265.
[11] Y. Gou, P. Chen, L. Yang, S. Li, L. Peng, S. Song, Y. Xu, Degradation of fluoroquinolones in homogeneous and heterogeneous photo-Fenton processes: a review, Chemosphere, 270 (2020) 129481, doi: 10.1016/j.chemosphere.2020.129481.
[12] S. Hussain, E. Aneggi, D. Goi, Catalytic activity of metals in heterogeneous Fenton-like oxidation of wastewater contaminants: a review, Environ. Chem. Lett., 19 (2021) 2405–2424.
[13] M. Ghorbanpour, Soybean oil bleaching by adsorption onto bentonite/iron oxide nanocomposites, J. Phys. Sci., 29 (2021) 113–119.
[14] N. Hajipour, M. Ghorbanpour, A. Feizi, Application of photo-Fenton dye removal with γ-Fe_2O_3/bentonite nanocomposites prepared by solid-state reaction in wastewater treatment, Desal. Water Treat., 233 (2021) 311–318.
[15] R. Shayegh, M. Ghorbanpour, A new approach for the preparation of iron oxide-pillared bentonite as adsorbent of dye, Desal. Water Treat., 183 (2020) 404–412.
[16] H.D. Rojas-Mantilla, S.C. Ayala-Duran, R.F. Pupo Nogueira, Modification of a Brazilian natural clay and catalytic activity in heterogeneous photo-Fenton process, Chemosphere, 291 (2021) 132966, doi: 10.1016/j.chemosphere.2021.132966.
[17] M.A. De León, M. Rodríguez, S.G. Marchetti, K. Sapag, R. Faccio, M. Sergio, J. Bussi, Raw montmorillonite modified with iron for photo-Fenton processes: influence of iron content on textural, structural and catalytic properties, J. Environ. Chem. Eng., 5 (2017) 4742–4750.
[18] M. Khatamian, B. Divband, R. Shahi, Ultrasound assisted co-precipitation synthesis of Fe_3O_4/bentonite nanocomposite: performance for nitrate, BOD and COD water treatment, J. Water Process. Eng., 31 (2019) 100870, doi: 10.1016/j.jwpe.2019.100870.
[19] A.A. Radhakrishnan, B.B. Beena, Structural and optical absorption analysis of CuO, Ind. J. Adv. Chem. Sci., 2 (2014) 158–161.
[20] H.B. Hadjltaief, M.B. Zina, M.E. Galvez, P. Da Costa, Photo-Fenton oxidation of phenol over a Cu-doped Fe-pillared clay, C.R. Chim., 18 (2015) 1161–1169.
[21] K. Bama, M. Sundrarajan, Improved surface morphology of silver/copper oxide/bentonite nanocomposite using aliphatic ammonium based ionic liquid for enhanced biological activities, J. Mol. Liq., 241 (2017) 1044–1058.
[22] F.H. AlHamedi, M.A. Rauf, S.S. Ashraf, Degradation studies of Rhodamine B in the presence of UV/H_2O_2, Desalination, 239 (2009) 159–166.
[23] M.S. Lucas, J.A. Peres, Decolorization of the azo dye Reactive Black 5 by Fenton and photo-Fenton oxidation, Dyes Pigm., 71 (2006) 236–244.
[24] M. Tariq, M. Muhammad, J. Khan, A. Raziq, M. Kashif Uddin, A. Niaz, S.S. Ahmed, A. Rahim, Removal of Rhodamine B dye from aqueous solutions using photo-Fenton processes and novel Ni-Cu@MWCNTs photocatalyst, J. Mol. Liq., 312 (2020) 113399, doi: 10.1016/j.molliq.2020.113399.